ARTICLE NO. 79-1747R

Pilot-Optimal Augmentation for the Air-to-Air Tracking Task

David K. Schmidt*
Purdue University, West Lafayette, Ind.

A method based on optimal control techniques, closed-loop task-oriented design objectives, and an optimal control model of the human pilot was applied to augment the system dynamics in a longitudinal air-to-air tracking task. The plant dynamics included not only the vehicle short-period mode but the dynamics of two different lead-computing sight displays at different racking ranges and levels of target acceleration. Previously obtained experimental results were duplicated, a family of full-state feedback linear control laws developed, tracking improvements predicted, and augmented system dynamics (eigenvalues) investigated. The results demonstrate the dependence of the desirable vehicle (short-period) dynamics on the dynamics of the other system modes (e.g., the display), thus emphasizing the importance of considering all of the system dynamics in handling qualities investigation and stability augmentation synthesis.

Nomenclature

A = plant matrix $(n \times n)$
A_P = augmented plant matrix $(n \times n)$
a_T = target plunge acceleration
B = control matrix $(n \times m)$
B_P = augmented control matrix $(n \times m)$
C = observation matrix $(l \times n)$
D = distance to target
E = expected value operator
F = augmentation control input weighting $(m \times m)$
G = pilot control input rate weighting $(m \times m)$
H = human describing function (matrix in OCM)
h = element in human describing function matrix
J = objective function
$K_{(\cdot)}$ = feedback gain for state $(\cdot)$
K_P = pilot describing function gain
M = Mach number
$M_{(\cdot)}$ = vehicle dimensional derivative-pitch acceleration due to $(\cdot)$
$M_{1\text{-}4}, N_{1\text{-}4}$ = transfer function numerator coefficients
n = dummy noise state variable
Q = output weighting $(l \times l)$
q = vehicle pitch rate
R = pilot control input weighting
s = Laplace parameter
T_f = projectile time of flight
T_L = pilot's lead-time constant
T_ϵ, T_λ = pilot's observation thresholds
u_{aug} = augmentation control vector, m
$\bar{u}_p$ = pilot control vector, m
V = flight velocity
$V_{(\cdot)}$ = variance of parameter $(\cdot)$ for pilot remnant
w = "white" stochastic process
$\bar{x}$ = state vector (n)
$\bar{y}$ = output vector (l)
$Z_{(\cdot)}$ = vehicle dimensional derivative-plunge acceleration due to $(\cdot)$
α = vehicle angle of attack
β = relative line-of-sight angle
γ_T = target flight path angle
Δ = variation
δ_E = elevator deflection angle
δ_{st} = stick deflection angle
ϵ = tracking error angle
$\zeta_{(\cdot)}$ = damping for mode $(\cdot)$
θ = vehicle pitch angle
θ_c = commanded angle
λ = displayed lead angle
$\rho_{(\cdot)}$ = ratio of remnant to variable $(\cdot)$ noise
$\sigma^2_{(\cdot)}$ = variance of the physical variable $(\cdot)$
τ = delay
τ_a = actuator time constant
τ_N = neuromuscular time constant
$\omega_{(\cdot)}$ = generic undamped natural frequency for mode $(\cdot)$

Received July 17, 1979; presented as Paper 79-1747 at the AIAA Guidance and Control Conference, Boulder, Colo., Aug. 6-8, 1979; revision received Dec. 11, 1979.

Index categories: Guidance and Control; Handling Qualities, Stability and Control; Human Factors.

*Associate Professor of Aeronautics and Astronautics. Associate Fellow AIAA.

Introduction

WITH the growing dynamic complexity of advanced flight vehicles (e.g., control-configured and/or highly flexible vehicles), the utility of conventional, open-loop, rigid-body handling qualities specifications for dynamic augmentation synthesis diminishes. An alternative design approach is to apply closed-loop task-oriented design objectives and include analytical representations of the pilot. Previously presented[1] was the initial development of an augmentation synthesis methodology that utilizes an optimal control model (OCM) of the human pilot[2] and applies optimal control laws compatible with the pilot's objectives and capabilities. Thus, the analysis approach is particularly suited to multidimensional high-order systems. Furthermore, to maximize pilot acceptance, the pilot's objective function in the human operator model is also used as the augmentation design objective function. The rationale for this latter feature stems from the high correlation between the resulting magnitude of the quadratic functional of the OCM and the actual pilot's subjective ratings obtained in experiments.[3] Finally, due to the cooperative structure of the pilot and augmentation, the method necessarily involves the simultaneous solution of two coupled optimal control problems.

In this paper, the problem to be addressed is the augmentation of the plant dynamics in an (air-to-air pitch) tracking task. The higher-order system dynamics actually include linearized flight vehicle rigid-body and actuator dynamics as well as the display dynamics of two lead-

computing sights. In each of the cases considered, the vehicle flight condition, and therefore rigid-body dynamics, remain unchanged. However, the sight dynamics vary considerably between cases with different sight types and tracking ranges.

The vehicle and one of the sights is identical to one of the cases addressed experimentally, as well as analytically (via the OCM), by Harvey.[4] In his investigation, Harvey used fixed-base simulation data to infer the pilot's objective function *in this task*. A unique objective function was found to yield extremely good correlation (in terms of rms statistics) between analytical and experimental results over a wide range of system dynamics. It is therefore assumed in our work here that this same objective function is invariant with the system dynamics, and is used in all cases considered.

The objectives of this investigation include not only the estimation of the performance improvement attainable with augmentation, but also, and perhaps more important, the determination of the most desirable plant or controlled-element dynamics. By parametrically varying the level of augmentation, we are able not only to establish trends in the desirable plant characteristics, but also the predicted changes in the human operator characteristics with varying high-order plant characteristics. Finally, the results so obtained are compared to those of Hollis,[5] who used simple pitch-rate and plunge-acceleration feedback along with Anderson's paper pilot[6] to determine optimum vehicle dynamics for pitch tracking with a fixed sight (with no display dynamics).

System Models

The vehicle dynamics are the linearized short-period approximation for a typical fighter aircraft in level flight at 15,000 ft altitude, Mach no. = 0.9 (V = 952 ft/s), and the specifics are presented in Table 1. Also, to aid in the interpretation of results, we will consider augmenting the simple, second-order plant ($\theta(s)/\delta_{st}(s) = K/s^2$).

The schematics of the displays are shown in Fig. 1. The tracking task, of course, involves the desire to minimize the tracking error ϵ, where for the simple K/s^2 plant

$$\epsilon = \theta - \theta_c$$

For the pitch tracking task,

$$\epsilon = \lambda - \beta$$

where β, the relative line-of-sight angle, is governed by the relations

$$\dot{\beta} = q - \frac{V}{D}(\gamma_T - \theta + \alpha) \qquad \dot{\gamma}_T = -\frac{1}{V}a_T$$

Note that for this display, the fixed reference mark represents the weapon line and the sight (reticle and pipper) is dynamic (moves in display).

For the high-order pitch-tracking task, the displayed variable, or lead angle λ, includes the lead required for velocities and accelerations, as well as a ballistic "jump" correction. The governing linearized equation of an ideal sight is

$$\lambda = T_f(\dot{\theta} - \dot{\beta}) - \frac{T_f^2}{2D}a_T - 0.038\frac{VT_f}{D}\alpha \qquad (1)$$

This relation implies that the line-of-sight rate $\dot{\beta}$ and the target's normal acceleration a_T are available for lead-angle calculation, and therefore represents an idealized sight. A second lead-angle equation representing an actual typical sight is given as

$$\dot{\lambda} = -\frac{1}{T_f}\lambda - \left(\frac{Z_\alpha T_f}{2D} + 0.038\frac{V}{D}\right)\alpha + \dot{\theta} \qquad (2)$$

Table 1 Vehicle math model

$\dot{\alpha}$	$= Z_\alpha\alpha + q + Z_\delta\delta_E$	τ_a	$= 0.05$ s
$\dot{\theta}$	$= q$	ζ_{SP}	$= 0.32$
$\dot{q}$	$= (M_\alpha + M_{\dot{\alpha}}Z_\alpha)\alpha + (M_q + M_{\dot{\alpha}})q + (M_\delta + M_{\dot{\alpha}}Z_\delta)\delta_E$	ω_{SP}	$= 3.35$ rad/s
		M_α	$= -10.4$ rad/s^2
$\dot{\delta}_E$	$= -(1/\tau_a)\delta_E + 16\delta_{\text{stick}}$	$M_{\dot{\alpha}}$	$= -0.344$ rad/s
Z_α	$= -983$ ft/s^2	M_q	$= -0.738$ rad/s
Z_δ	$= -90.5$ ft/s^2	M_δ	$= -37.1$ rad/s^2

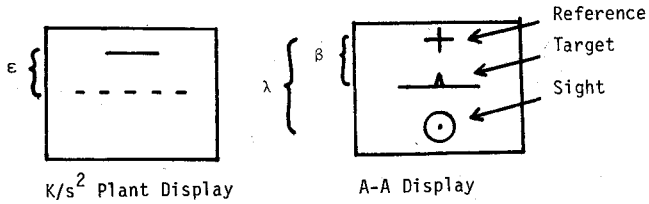

Fig. 1 Display schematics.

This relation is obtained from the above by assuming that the line-of-sight rate $\dot{\beta}$ may be approximated by the lead-angle rate $\dot{\lambda}$, and the target acceleration is approximately equal to the attacker's, or $a_T \simeq Z_\alpha\alpha$. Note that since the actual sight [Eq. (2)] depends entirely on the attacker's variables (α, θ, etc.), it is much more sensitive to pilot stick input than the ideal sight. Also note the sight dynamics are clearly a function of tracking range. Two tracking ranges were considered, D = 1000 ft and D = 3000 ft, associated with two projectile times of flight, T_f = 0.33 s and T_f = 1.30 s, respectively. The process driving noise for the pitch tracking case is the target normal acceleration generated by filtered white noise where

$$\dot{a}_T = -0.33a_T + n \qquad \dot{n} = -0.33n + w(t)$$

and the white noise intensity is selected to yield chosen levels of target accelerations. The driving noise for the K/s^2 plant is simply the commanded variable θ_c generated by filtered white noise where

$$\ddot{\theta}_c + a\dot{\theta}_c + b\theta_c = w(t)$$

For comparison purposes, the transfer functions for the three systems are given in Table 2. The numerator coefficients N_1-N_4 and M_1-M_4 are functions of vehicle and sight characteristics, and therefore depend on tracking range or, equivalently, T_f. On the other hand, except for the sight time constant T_f in the typical-sight case, the denominator is a function of vehicle characteristics alone.

The optimal control model (OCM) of the pilot[2] assumes that the well-trained well-motivated human operator chooses his control inputs $\dot{u}_p$, subject to human limitations, such that the following objective function is minimized:

$$J_p = E\left\{\lim_{T\to\infty}\frac{1}{T}\int_0^T (\bar{y}'Q\bar{y} + \bar{u}_p'R\bar{u}_p + \dot{\bar{u}}_p'G\dot{\bar{u}}_p)\,dt\right\} \qquad (3)$$

and G is selected to obtain a chosen neuromuscular lag time constant τ_N. The pilot's input is then expressed in the scalar case as

$$\tau_N\dot{u}_p = -K_x\hat{x} - u_p$$

The selected parameters of the model in this investigation are given in Table 3, and are consistent with those in Harvey's[4] investigation of this task. (Note that nominal values of model parameters have been chosen which do not reflect the pilot's acceleration environment. This was done to be consistent with fixed-base simulation results.)

Table 2 Transfer function comparison

Second-order plant

$$\epsilon(s)/\delta_{st}(s) = 11.7/s^2$$

Ideal sight display (Eq. 1)

$$\frac{\epsilon(s)}{\delta_{st}(s)} = \frac{K(N_1 s^3 + N_2 s^2 + N_3 s + N_4)}{s^2(\tau_a s+1)(s^2 + 2\zeta_{sp}\omega_{sp} s + \omega_{sp}^2)}$$

Typical sight display (Eq. 2)

$$\frac{\epsilon(s)}{\delta_{st}(s)} = \frac{K(M_1 s^3 + M_2 s^2 + M_3 s + M_4)}{s^2(T_f s+1)(\tau_a s+1)(s^2 + 2\zeta_{sp}\omega_{sp} s + \omega_{sp}^2)}$$

$$K = -16\tau_a/D$$

$$N_1 = -0.962 Z_\delta T_f$$

$$N_2 = (D/V + T_f)(VM_\delta + Z_\delta M_{\dot\alpha}) - Z_\delta$$

$$N_3 = Z_\delta(M_q + M_{\dot\alpha}) + (D/V + T_f)(M_\alpha Z_\delta - Z_\alpha M_\delta)$$

$$N_4 = M_\alpha Z_\delta - Z_\alpha M_\delta$$

$$M_1 = Z_\delta T_f(Z_\alpha D/2V^2 - 0.962)$$

$$M_2 = N_2 + T_f(Z_\alpha D/2V^2 - 0.962)(VM_\delta - M_q Z_\delta)$$

$$M_3 = N_3$$

$$M_4 = N_4$$

Table 3 Pilot model parameters

Observation delay	$\tau = 0.2$ s
Neuromuscular time constant	$\tau_N = 0.1$ s
Observed variables	$\bar{y}' = [\epsilon, \dot\epsilon, \lambda, \dot\lambda]$
Cost function weightings	$Q_{y_{ii}} = [16, 1, 0, 4]$ $R_u = 0$
Observation thresholds	$T_\epsilon = T_\lambda = 0.65$ deg $T_{\dot\epsilon} = T_{\dot\lambda} = 1.3$ deg/s
Observation noise variance	$V_{yi} = \pi\rho_y\sigma_y^2$, $\rho_y = 0.01$
Motor noise variance	$V_{u_p} = \pi\rho_u\sigma_{u_p}^2$, $\rho_u = 0.001$

Table 4 Performance comparison

	Parameter (rms)			
	ϵ, deg	λ, deg	q, deg/s	δ_E, deg
		$D = 1000$ ft		
Experiment	2.1	2.9	8.0	2.1
Analytical (typical sight)	2.3	2.9	8.7	2.1
Analytical (ideal sight)	1.6	2.6	7.9	2.0
		$D = 3000$ ft		
Experiment	2.4	8.7	6.4	1.8
Analytical (typical sight)	2.3	10.1	7.3	1.8
Analytical (ideal sight)	1.1	9.7	6.0	1.6

$\sigma_{a_T} = 3.5$ g's for all cases.

Shown in Table 4 is the predicted (rms) performance using this OCM as compared with Harvey's (fixed-base simulator) experimental results[4] for the typical sight display. Also shown is the predicted performance for the idealized sight for reference.

System Augmentation

With the above system models, we represent the system, including the pilot's control input as well as the augmentation input, by the relation

$$\dot{\bar{x}} = A\bar{x} + B\bar{u}_p + B\bar{u}_{\text{aug}} + \bar{w}$$

where u_{aug} is an equivalent stick input—in this case a scalar. As shown previously,[1] if $\bar{u}_{\text{aug}}$ is chosen to minimize the objective function

$$J_{\text{aug}} = J_p + E\left\{\lim_{T\to\infty}\frac{1}{T}\int_0^T \bar{u}'_{\text{aug}} F \bar{u}_{\text{aug}}\,dt\right\} \quad (4)$$

where J_p is given in Eq. (3), the relation for the augmentation input is

$$\bar{u}_{\text{aug}} = -F^{-1}B'K_{A_1}\bar{x} - F^{-1}B'K_{A_2}\bar{u}_p$$

or

$$\bar{u}_{\text{aug}} = -K_x\bar{x} - K_u\bar{u}_p$$

(The matrices K_{A1} and K_{A2} are obtained, as discussed in Ref. 1, by simultaneously solving two coupled Riccati equations—one yielding the augmentation gains, and one yielding the pilot's gains.)

The result, of course, is the pilot controlling the augmented system, which is now described by

$$\dot{\bar{x}} = (A - BK_x)\bar{x} + B(I - K_u)\bar{u}_p + \bar{w}$$

or

$$\dot{\bar{x}} = A_p\bar{x} + B_p\bar{u}_p + \bar{w}$$

Second-Order Plant

Let us initially consider the effects of pilot optimal augmentation of the second-order plant for which we may define $\bar{x}' = (\theta_c, \dot\theta_c, \theta, \dot\theta)$ and $\bar{y}' = (\epsilon, \dot\epsilon)$. Shown in Fig. 2 is the augmented open-loop and pilot closed-loop root locus obtained via optimal augmentation for various u_{aug} objective-function weights, or F in Eq. (4). (A-E indicate open- and closed-loop cases with increasing augmentation.) Note the shape of the augmented (open-loop) system root locus, as well as that of the pilot closed-loop system corresponds to the known[7] asymptotic behavior of the closed-loop roots of a linear optimally controlled single-input single-output system. In this case, the root locus assumes a Butterworth configuration of order two. (This results from two open-loop

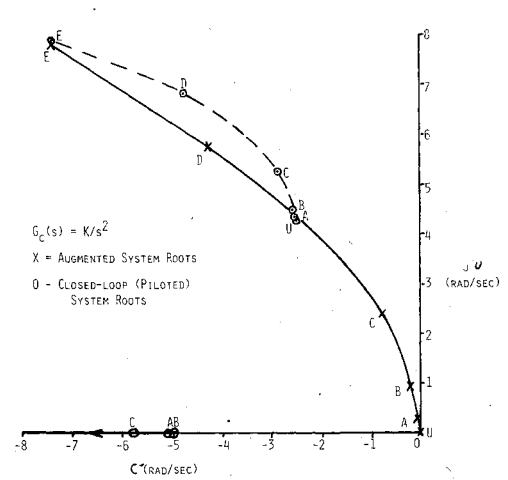

Fig. 2 Second-order plant root loci.

plant poles and no zeros, except the pilot closed-loop poles include a third, introduced via the pilot's neuromuscular lag.)

The distance between open- and closed-loop eigenvalues is a maximum for no augmentation (i.e., $F \to \infty$), while the open- and closed-loop poles coalesce for increasing augmentation, eventually eliminating the pilot compensation, and the system monotonically approaches a pure automatically controlled system.

To aid in further interpretation of these results, consider the human operator describing function[8] in a compensatory task to be approximated by

$$H(s) = \frac{K_p e^{-\tau s}(T_L s+1)}{(\tau_N s+1)}$$

or a gain, low-frequency lead, effective delay, and neuromuscular lag. Our augmented or unaugmented second-order plants may be described in general by the transfer function

$$G(s) = K/(s^2+2\zeta\omega s+\omega^2)$$

The piloted closed-loop denominator now becomes (ignoring the delay)

$$s^3+\left(\frac{1}{\tau_N}+2\zeta\omega\right)s^2+\left[\omega^2+\frac{1}{\tau_N}(2\zeta\omega+KK_pT_L)\right]s + \frac{1}{\tau_N}(\omega^2+KK_p)$$

If we write this closed-loop denominator as

$$(T_c s+1)(s^2+2\zeta_c\omega_c s+\omega_c^2)$$

or

$$s^3+\left(\frac{1}{T_c}+2\zeta_c\omega_c\right)s^2+\left(\omega_c^2+\frac{1}{T_c}2\zeta_c\omega_c\right)s+\frac{1}{T_c}\omega_c^2$$

we see that the pilot's gain K_p is related to the difference between open- and closed-loop frequencies by the relation

$$KK_p = (\tau_N/T_c)\omega_c^2-\omega^2$$

Therefore, the pilot's gain tends to be proportional to the difference between the squares of closed- and open-loop natural frequencies, or equivalently, the squares of distances of the poles from the origin.

Also, the pilot's lead T_L is related to the open- and closed-loop parameters by the relation

$$T_L = \frac{\tau_N[(\omega_c^2-\omega^2)+2(\zeta_c\omega_c/T_c-\zeta\omega/\tau_N)]}{(\tau_N/T_c)\omega_c^2-\omega^2}$$

Therefore, the pilot's lead would tend to increase with increasing $\Delta(\zeta\omega)/\Delta\omega^2$ between open- and closed-loop eigenvalues. With three observations, we are able to qualitatively relate the trends from the root locus (Fig. 2) to the parameters in the classical human operator describing function.

In the case of higher-order systems, however, the pilot describing function may not be well approximated by the simpler forms, and the relationships between the root locus characteristics and the predicted human describing function parameters are much more complex and difficult to express quantitatively. Still, the effects of augmentation and of the pilot's gains are depicted in the root loci, and the difference between the open- and closed-loop roots indicate, at least qualitatively, the required level of human equalization involved. Finally, the augmented (open-loop) system root locus yields important information about the desirable trends in the system's dynamics.

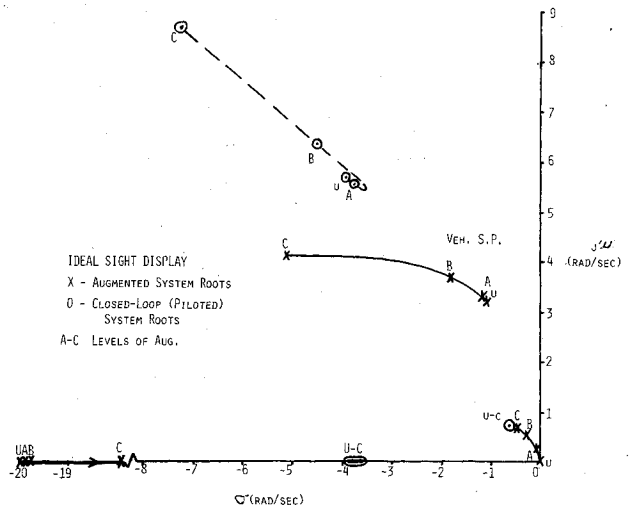

Fig. 3 Ideal display root loci.

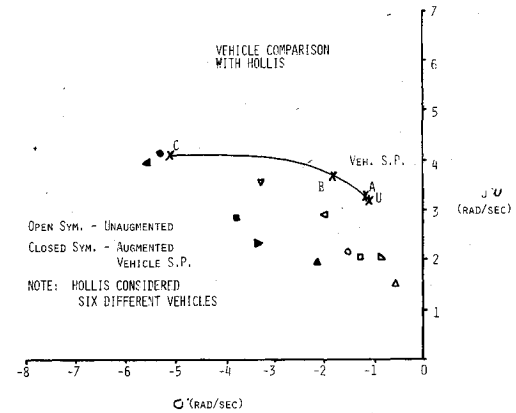

Fig. 4 Vehicle dynamics comparison.

Ideal Sight Display

Consider now, the optimal augmentation of the air-to-air tracking task with the system including the ideal sight display [lead angle obtained from Eq. (1)]. Again, with decreasing augmentation control input weight [F in Eq. (4)], we generate a family of augmented systems. The open- and closed-loop eigenvalues are shown in Fig. 3.

The open-loop roots include in the unaugmented case, the two roots at the origin, the vehicle short-period roots, and the actuator root at -20 rad/s.

For the piloted closed-loop system, still unaugmented, the roots include a low-frequency pair, a high-frequency pair, and two real roots, one at -3.7 rad/s and one (not shown for clarity) at -20 rad/s.

As the level of augmentation is increased, as indicated by cases A-C, the frequency and damping of the vehicle short-period mode is increased and the two poles originally at the origin move toward the piloted closed-loop low-frequency pair due to the closure of the tracking loop (i.e., feedback of ϵ and $\dot{\epsilon}$). With the pilot closing the loop on the augmented systems, a unique pair of high-frequency roots are associated with each level of augmentation, and this pair appears to follow a Butterworth pattern. However, for the levels of augmentation considered, the two real closed-loop roots (at approximately -20 and -3.7 rad/s) are relatively insensitive to augmentation level. Also, the low-frequency pair (at about $-0.7 \pm 0.7j$) are invariant with augmentation. This pair also corresponds closely to a pair of plant zeros.

This behavior is consistent with the asymptotic properties of linear optimally controlled system roots cited previously. For single-input single-out systems, p of the roots tend toward the p open-loop zeros (in the left half-plane), and the

remaining roots assume a Butterworth configuration of order $n-p$. Furthermore, the systems with input and output vectors of equal dimension (i.e., systems with square transfer-function matrices), p of the closed-loop roots tend to the p "zeros" of the determinant of the transfer function matrix. Although, the transfer function matrix is not square in this case, the invariance of any closed-loop roots may still be explained in terms of the above properties and the existence of system "pseudo-zeros."

Shown in Fig. 4 is the comparison of these (vehicle short-period) results with those of Hollis.[5] In his analysis, Hollis determined the vehicle augmentation yielding the best pilot rating via the "paper-pilot."[6] Pitch rate and plunge acceleration were used for augmenting only the vehicle with a fixed sight (with no display dynamics). It is seen that the results agree with the trend determined by Hollis' consideration of several sets of vehicle dynamics. In all cases, the "optimal" augmentation increased the frequency and damping of this vehicle mode. This trend, as noted by Hollis, also agrees with the military specifications on flying qualities.[9] (As we shall see later, this is not the case for the other sight display.)

The predicted improvement in (rms) tracking accuracy for the ideal sight is shown in Table 5, along with the rms statistics on stick deflection and rate of deflection, i.e., physical workload. Recall that the stick deflection was not considered penalized in the pilot's objective function, hence little reduction in this parameter is obtained through augmentation. However, rms stick rate is significantly reduced.

Finally, Table 6 lists the optimum full-state feedback gains in this idealized case for each level of augmentation.

For this sight display, increasing the tracking range D from 1000 to 3000 ft changed the results very slightly. The feedback gains varied approximately 15% and the augmented and piloted system root loci were almost identical to that in Fig. 3. The position of the invariant low-frequency piloted-system roots did change from $-0.7 \pm 0.7j$ to -0.3 and -1.2 rad/s, but the augmentation moved the poles at the origin toward those roots as in the 1000 ft case.

Typical Sight Display

Considering now the system with the more typical display dynamics [lead angle computed with Eq. (2)], the open- and closed-loop root loci are shown in Fig. 5. The unaugmented system roots in this case include those considered above plus the lead-angle time constant T_f. Comparing these results with those in Fig. 3, we see an entirely different trend in the vehicle short-period roots! With the more sensitive, or "active," sight display in this case, the optimum short-period frequency remains relatively constant while the damping is increased.

Table 5 Augmented performance (rms)

	Unaugmented	Level A	Level B	Level C
Error ϵ, deg	1.92	1.71	0.95	0.35
Deflection δ, deg	3.61	3.55	3.50	3.55
Rate $\dot{\delta}$, deg/s	7.16	6.25	5.39	4.87

$\sigma_{A_T} = 5\,g$'s, $D = 1000$ ft.

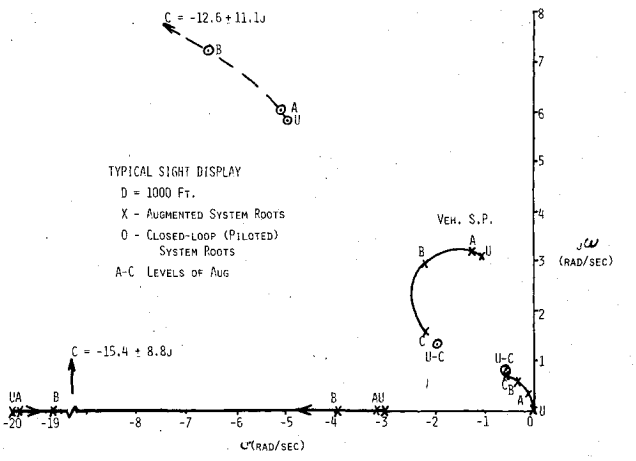

Fig. 5 Actual sight root loci ($D = 1000$ ft).

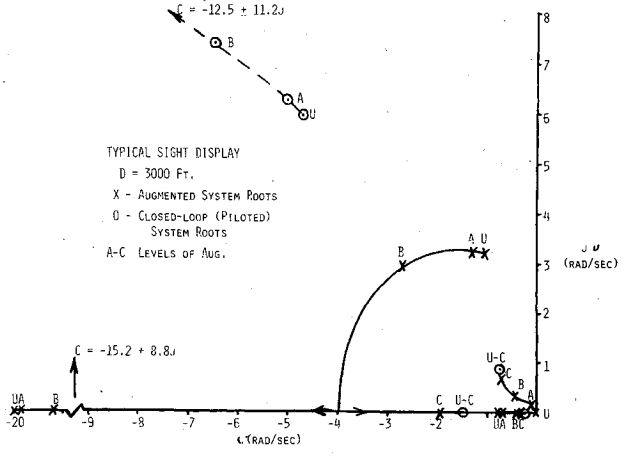

Fig. 6 Actual sight root loci ($D = 3000$ ft).

Recall that the results obtained by Hollis included no display dynamics, and that the results agreed with those obtained with the less active, ideal sight display. Additionally, the augmented short-period roots in the case considered here (Fig. 5) approach an invariant pair of piloted closed-loop eigenvalues, a trend not observed in the ideal-sight case.

The behavior of the roots near the origin is as observed previously: the augmentation closing the tracking loop and moving the plant poles at the origin toward the two invariant closed-loop eigenvalues. Also, the actuator and sight time constants move together, due to augmentation, and eventually become a high-frequency complex pair. Finally, as before, a unique high-frequency closed-loop pair is associated with each level of augmentation, and approaches a Butterworth pattern. A seventh closed-loop root at -20 rad/s is introduced by the pilot's neuromuscular lag, but is not shown for clarity.

Increasing the range to the target D from 1000 to 3000 ft results in the root loci shown in Fig. 6. Now, not only do the plant zeros (and therefore the "pseudo-zeros") depend on D, but the sight time constant T_f is affected as well. As a result, this root locus is appreciably different from that in Fig. 5,

Table 6 Optimum gains—ideal sight display

Augmentation level	K_n	K_{a_T}	K_{γ_T}	K_β	K_α	K_θ	K_q	K_{δ_E}	$K_{\delta_{st}}$
A	-0.113×10^{-5}	-0.735×10^{-5}	0.021	0.030	0.030	−0.051	−0.011	0.017	0.029
B	-0.725×10^{-5}	-0.492×10^{-4}	0.144	0.213	0.189	−0.357	−0.072	0.111	0.154
C	-0.267×10^{-4}	-0.206×10^{-3}	0.632	0.995	0.734	−1.63	−0.314	0.432	0.383

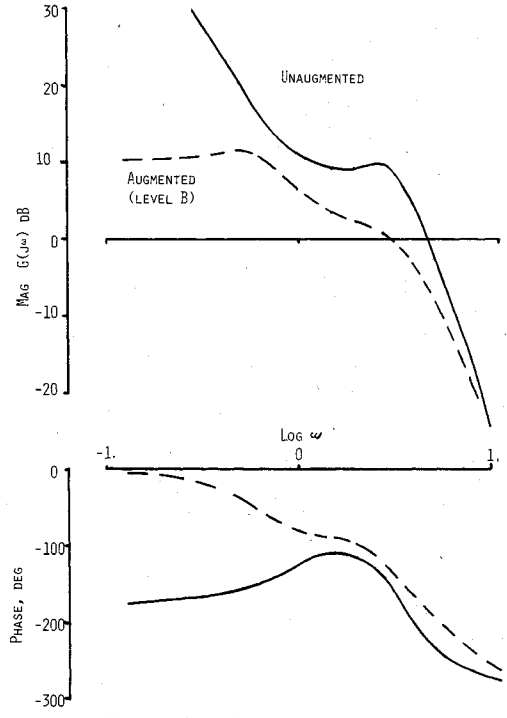

Fig. 7 Plant frequency response.

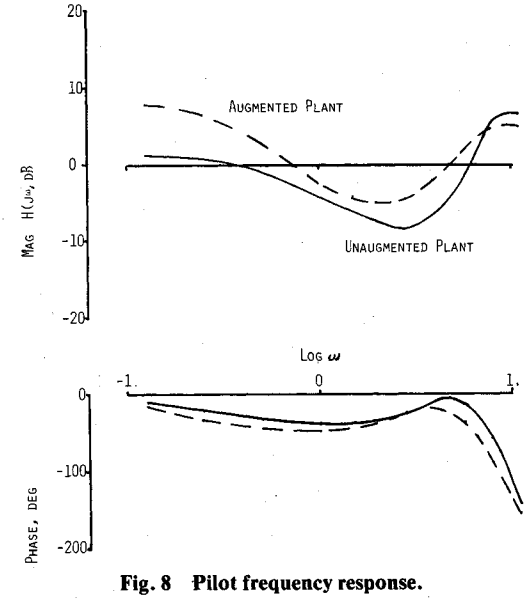

Fig. 8 Pilot frequency response.

particularly at the higher level of augmentation. Still present, however, are the four invariant closed-loop poles—two real and two complex in this case—and the family of complex closed-loop roots at the higher frequency. Note in this case, the migration of the sight time constant with augmentation toward the closed loop root at -0.3 rad/s and the behavior of the augmented short-period roots for level C.

The effect of augmentation (level B, $D=1000$ ft) on the system's frequency response (ϵ/δ) is depicted in Fig. 7.

Table 7 Augmented performance (rms)

	Unaugmented	Level A	Level B	Level C
Error ϵ, deg	3.05	2.50	1.12	0.31
Deflection δ_{st}, deg	3.71	3.64	3.51	3.68
Rate $\dot{\delta}_{st}$, deg/s	7.33	6.64	5.36	5.10

$\sigma_{A_T}=5\,g$'s, $D=1000$ ft.

Closure of the tracking loop (via ϵ and $\dot{\epsilon}$ feedback) eliminates the $1/s^2$ characteristic at low frequency, while the increased damping of the short-period mode at $\omega\simeq 3$ rad/s) is evident. The effect of this level of augmentation on the predicted frequency response of the pilot is shown in Fig. 8. With augmentation, the pilot appears to increase his gain, as well as adding slightly more low-frequency lag. Also, his required lead near $\omega=3$ rad/s would appear to be decreased.

The pilot frequency response shown in this figure is that of an equivalent describing function formed from the transfer function matrix ($H(s)$) obtained from the optimal control pilot model. This equivalent describing function is analogous to the classical human describing function measured experimentally in a compensatory task, and is obtained from the relation

$$\left.\frac{\delta_{st}(s)}{\epsilon(s)}\right|_{\text{equiv.}}=\frac{\delta_{st}(s)}{\epsilon(s)}+s\frac{\delta_{st}(s)}{\dot{\epsilon}(s)}=h_{i1}(s)+sh_{i2}(s)$$

where $\delta_{st}(s)=H(s)\bar{y}(s)$.

The effect of the augmentation on the predicted rms performance is shown in Table 7. The rms error ϵ, stick deflection, and stick rate are given for $D=1000$ ft, $\sigma_{aT}=5\,g$'s. Here again we see a significant improvement in tracking error, while the rms stick activity remains approximately constant with increased augmentation. As before, however, we note that stick activity was not penalized in the objective functions. The pilot stick rate is also reduced with augmentation.

The above improvements in tracking accuracy were obtained, while the predicted elevator activity actually decreased slightly with increased augmentation (2.96 deg-rms unaugmented to 2.81 deg-rms for level C). This is due to the fact that the augmentation includes pilot stick position feedback $K_{\delta_{st}}$ so the *net* commanded elevator deflection by the pilot beomes

$$\delta_E=K(1-K_{\delta_{st}})\delta_{st}$$

where K is the actual stick gain. With his effective stick gain reduced, the pilot's contribution to commanded elevator is reduced, while the augmentation's contribution is increased. The sum of the two results in the relatively constant net rms elevator with increasing augmentation. The optimum gains for the vehicle states for the three levels of augmentation is given in Table 8.

Conclusions

In this effort, we have applied an optimal control approach, including an optimal control model of the human

Table 8 Optimum gains—typical sight

1000 ft	K_n	K_{a_T}	$K_{\gamma T}$	K_β	K_λ	K_α	K_θ	K_q	K_{δ_E}	$K_{\delta_{st}}$
$F^{-1}=0.001$	-0.138×10^{-5}	-0.952×10^{-5}	0.027	0.037	0.014	0.042	-0.065	-0.180	0.029	0.044
$F^{-1}=0.01$	-0.819×10^{-5}	-0.590×10^{-4}	0.176	0.246	0.102	0.245	-0.442	-0.122	0.185	0.211
$F^{-1}=0.1$	-0.298×10^{-4}	-0.236×10^{-3}	0.731	1.07	0.493	0.872	-1.80	-0.535	0.689	0.467

pilot and closed-loop performance objectives, to investigate the augmentation of a tracking task with high-order system dynamics. The method is well-suited for multivariable systems analysis, and as such provides an alternative to model-following synthesis techniques. It could also be used in conjunction with following techniques since the pilot-optimal augmentation method used here provides the insight into the desirable augmented system dynamics via the open- and closed-loop system root loci.

When considering augmenting the second-order plant, we were able to easily relate the effects of augmentation to changes in the approximate human describing functions frequently used. However, in the case of high-order systems, closed-loop analytical relations are unlikely. Therefore, the open- and closed-loop root locus and the frequency response obtained in our analysis approach are utilized for determining changes in not only the plant but the human operator as well.

Also noted was the agreement between the root loci patterns and the asymptotic behavior of the roots of an optimally controlled system. Since the transfer function matrices were not square in the two sight cases, the existence of plant pseudo-zeros was inferred from the presence of a number of invariant closed-loop poles toward which the augmentation moved the plant roots.

In the analysis of the higher-order systems, it was shown that the display dynamics affected the desirable vehicle (short-period) characteristics. These characteristics for a less "active" sight display were found to agree with those obtained elsewhere for a fixed sight. However, the short-period mode was modified differently with the more dynamic, typical sight display. The effect of other dynamic modes, such as structural, may have a similar effect and could be investigated with this same appraoch.

Finally, the predicted reduction in rms tracking error and pilot workload (in terms of rms stick rate) would appear to be significant. If these performance improvements could be realized, pilot rating would drastically improve.

Acknowledgments

The author would like to express his appreciation to S. N. Prasad who obtained many of the numerical results presented. This work was performed with the cooperation of the Flight Control Division, Air Force Flight Dynamics Laboratory, Wright-Patterson AFB, Ohio. It was supported under Contract AFOSR F44620-76-C-0052 and under Grant AFOSR-79-0042.

References

[1]Schmidt, D.K., "Optimal Flight Control Synthesis Via Pilot Modeling," *Journal of Guidance and Control,* Vol. 2, July-Aug. 1979, pp. 308-312.

[2]Kleinman, D.L., Baron, S., and Levison, W.H., "An Optimal Control Model of Human Response, Parts I and II," *Automatica,* Vol. 6, 1970, pp. 357-383.

[3]Hess, R.A., "Prediction of Pilot Opinion Ratings Using an Optimal Pilot Model," *Human Factors,* Vol. 19, No. 5, 1977, pp. 459-475.

[4]Harvey, T.R., "Application of an Optimal Control Pilot Model to Air-to-Air Combat," Air Force Institute of Technology M.S. Thesis, Wright-Patterson AFB, Ohio, GA/MA/74M-1, March 1974.

[5]Hollis, T.L., "Optimal Selection of Stability Augmentation System Parameters to Reduce the Pilot Ratings for the Pitch Tracking Task," Air Force Institute of Technology M.S. Thesis, Wright-Patterson AFB, Ohio, GGC/EE/71-10, June 1971.

[6]Anderson, R.O., "A New Approach to the Specification and Evaluation of Flying Qualities," Wright-Patterson AFB, Ohio, AFFDL-TR-69-120, Dec. 1969.

[7]Kwakernaak, H. and Sivan, R., *Linear Optimal Control Systems,* Wiley and Sons, Inc., New York, 1972, Sec. 3.8.

[8]McRuer D.T. and Krendel, E.S., "Mathematical Models of Human Pilot Behavior," NATO AGARDograph-AG-188, Jan. 1974.

[9]Anon., Military Specification, "Flying Qualities of Piloted Airplanes," MIL-F-8785B (ASG), 1969.